

WAVE PACKETS SCATTERED BY NON-PERIODIC BRAGG-TYPE LAYERED STRUCTURES

**Valentine F. Borulko, Oleg O. Drobakhin,
and Dmitry V. Sidorov***

Department of Physics, Electronics and Computer Systems, Oles Honchar National University of Dnepropetrovsk, 72, Gagarin Ave., Dnepropetrovsk 49010, Ukraine

Abstract—The time delay, space shift and widening of wave packet transmitted and reflected by structures with Bragg mirrors have been investigated. The specific structures such as Bragg mirrors, resonators, and structures with chirp variation of thickness of the “period” have been considered. The calculation has been carried out under the conditions that carrier frequency, and incidence angle is in the vicinity of the Bragg resonance. Integral (mass center) and differential (group) estimates of the delay time and space shift have been compared. The conditions for the appearance of anomalous (negative) mass center delay or mass center shift (Goos-Hänchen shift) of the reflected wave packet have been determined. The shape transformations of the wave packet illuminating periodic and quasiperiodic apodized Bragg reflectors have been under consideration. Spatial apodization of permittivity contrast yields much smaller shape deformation of the transmitted wave packet upon incidence at angles and carrier frequency near the edges of reflection band, as well in Bragg reflection band, in comparison with phenomena in similar periodic structures. The values of group delay for layered structures with a small chirp variation of optical (electrical) thickness of the period along longitudinal coordinates have been experimentally obtained in microwave range.

Received 5 March 2013, Accepted 13 May 2013, Scheduled 23 May 2013

* Corresponding author: Dmitry V. Sidorov (sidorov@email.ua).

1. INTRODUCTION

The structure periodicity is inherent to many media in nature. The trivial properties of reflection and transmission of electromagnetic waves under periodic structures irradiation are well known, being used in a wide range of applications [1–4]. In case of periodicity perturbation, the Bragg reflection becomes more complicated and gains great practical value [5]. The step disturbance of phase of periodic parameters results in a high quality eigen oscillation within the Bragg reflection bandwidth [6, 7]. The smooth perturbation of the amplitude of periodic parameters can ensure relative decrease of the quality factor of collateral resonance frequencies (these being outside the Bragg reflection band). For small numbers of Bragg reflection frequencies, we may achieve relative decrease of the quality factor of parasitic resonances by introducing small linear phase perturbation of periodicity parameter. The Bragg structures with spatially varied optical (electrical) thickness of the “period” are called chirped mirrors. The unit cell of two adjacent layers is considered as “period” of the structure. These structures are well known and widely applied in sources of ultra-short laser pulses to compensate the group delay dispersion (GDD) [8].

Based on applied problems, we have to consider the wave packets being some group of waves rather than a plane monochromatic wave. In this case, it is reasonable to consider the packets carrying the information, i.e., the signals [9]. The packets are strictly limited in time and space.

Propagation of packets in a medium, their reflection and transmission through structures are always accompanied by distortions via dispersion which can be neglected only within specified frequency and incident angle intervals for some certain propagation times and ranges. The dispersion phenomena are related with the proximity between the parameters of media or structures and the parameters of an electromagnetic wave. For the media, such parameters are distances between the energy states of atoms, molecules; whereas in structures, such parameter is the period. The normal and anomalous dispersion regions are distinguished by the sign of derivative of the refractive index (reflectivity phase). Nonequilibrium media with amplification usually have the negative dispersion [10].

The investigation of transformation of wave packets form with increasing the number of media boundaries becomes more complicated. If the permittivity and/or permeability slowly changes from layer to layer, the expressions that relate forms of the incident and transmitted packets can be obtained analytically using approximate methods of

solution of the Helmholtz equation [11]. For the rigorous calculation of the shape of the reflected and transmitted packets we have to use either the recurrence relations [12] or the transmission matrix method [13], which allow obtaining numerical values of the amplitudes of the field at the boundaries of layered structures. The presence of anisotropy and chirality additionally complicates form of the spatial distribution of the amplitude and polarization characteristics of the scattered packets [14]. Under oblique incidence the shift of reflected wave packet can be observed (Goos-Hänchen shift). Generally, magnitude of the shift is comparable with the wavelength at carrier frequency of the incident packet; however, with approaching the incident wave frequency to the resonant frequency of the medium with the permittivity dispersion the value of the shift may increase by orders, while near the Brewster angle negative values can be obtained [15]. In the most cases the anomalous (negative) values of lateral shift are caused by dispersion of material parameters [16], but in Bragg layered structures the anomalous values of lateral shift occur due to constructive interference [2].

The propagation, reflection and transmission of wave packets with the spectrum central frequency lying near one of the eigenfrequencies of media or structures cannot be analyzed just in terms describing the pulse as a whole (its velocity, shift, delay time). The packet widening and distortion should also be estimated, as well as specific limits, where the characteristics maintain physical meaning.

In this paper, we consider the reflection and transmission of wave packets for quasiperiodic apodized Bragg reflectors, symmetric and asymmetric resonators in the vicinity of the frequency and incidence angle of Bragg resonance, structures with linear modulation of the "period" thickness (chirp structures). Integrated (energy) and differential (group) estimates for time delay and the shift value will be compared.

Dependences of the skewness and kurtosis of the reflected wave packet versus carrier frequency in the Bragg reflection band for chirp structures will be calculated. Conditions for negative time delay and the magnitude of the shift of the reflected wave packets will be under consideration. The experimentally obtained values of group delay for layered structures with a small linear variation of optical (electrical) thickness of the period along the longitudinal coordinate will be presented.

2. METHODS OF INVESTIGATION

2.1. Transmission Matrix Method

In the formal description of the method of transmission matrices for electromagnetic wave propagation in multilayer structures, any isotropic homogeneous layer can be described by the second order square matrix which associates electric and magnetic field components on the boundaries of one layer [13]. The transmission matrix expression which holds for the case of thermal losses and materials with negative permittivity and permeability is of the form:

$$\mathbf{M}_j = \begin{pmatrix} \cos(k_{zj}h_j) & \frac{i}{p_j} \sin(k_{zj}h_j) \\ ip_j \sin(k_{zj}h_j) & \cos(k_{zj}h_j) \end{pmatrix} \quad (1)$$

where h_j is the geometric thickness of j -th layer, and ε_j and μ_j are the j -th layer permittivity and permeability. θ is the wave incidence angle in XOZ plane, k_0 the wave number of free space, and $k_{zj} = k_0 \sqrt{\varepsilon_j \mu_j - \sin^2 \theta}$ the longitudinal wave number. It is assumed that the direction of stratification coincides with the z axis. The p_j parameters are determined by the following expressions for TE and TM polarizations, respectively

$$p_j^{TE} = k_{zj} / (\mu_j k_0) = \sqrt{\varepsilon_j \mu_j - \sin^2 \theta} / \mu_j,$$

$$p_j^{TM} = k_{zj} / (\varepsilon_j k_0) = \sqrt{\varepsilon_j \mu_j - \sin^2 \theta} / \varepsilon_j.$$

For TE polarization, vector H lies in XOZ -plain, and vector E is perpendicular to this plain, but for TM polarization vector E lies in XOZ -plain, and vector H is perpendicular to it.

The resulting characteristic matrix \mathbf{M} of a layered structure is determined by the product of characteristic matrices of separate layers of the structure [1, 13]. Using the matrix components yields the expressions for the structure reflection R and transmission T coefficients, viz.

$$R(\omega, k_x) = \frac{[m_{11}(1-\Gamma) + m_{12}p_l(1+\Gamma)]p_1 - [m_{21}(1-\Gamma) + m_{22}p_l(1+\Gamma)]}{[m_{11}(1-\Gamma) + m_{12}p_l(1+\Gamma)]p_1 + [m_{21}(1-\Gamma) + m_{22}p_l(1+\Gamma)]} \quad (2a)$$

$$T(\omega, k_x) = \frac{2p_1}{[m_{11}(1-\Gamma) + m_{12}p_l(1+\Gamma)]p_1 + [m_{21}(1-\Gamma) + m_{22}p_l(1+\Gamma)]} \quad (2b)$$

where m_{uv} is the u -th line element in v -th column of the resulting transmission matrix, Γ the reflection coefficient of a structure load,

and p_l the parameter of the material of the last structure's layer (or of the half-space in case of $\Gamma = 0$). If a layered structure ends with a metal plane, then $|\Gamma|$ is equal to 1. Hereinafter, the normalized frequency f/f_0 dependence will be used, where f_0 means the first Bragg resonance frequency. Because dielectric materials ($\mu_1 = \mu_2 = 1$) will be under consideration, f_0 should be represented in following form of $f_0 = c/(2(h_1\sqrt{\varepsilon_1} + h_2\sqrt{\varepsilon_2}))$, where $h_1\sqrt{\varepsilon_1}$ and $h_2\sqrt{\varepsilon_2}$ are electrical thicknesses of layers of a structure period, c is the speed of light in vacuum.

2.2. Group Shift and Delay of Wave Packets

To analyze the wave packets shape transformation, let us use the Fourier integral representation. This approach provides that all incident, reflected and transmitted waves are a superposition of plane harmonic waves with different frequency and angle of incidence. The spectrum of the incident packet $F(\omega, k_x)$ can be obtained from the amplitude distribution $f(\tau, x)$ with the direct Fourier transform [9, 13, 17]:

$$F(\omega, k_x) = \int_{-\infty}^{\infty} \int_{-\infty}^{\infty} f(\tau, x) \exp(-i\omega\tau + ik_x x) d\tau dx.$$

where ω is the cyclic frequency and k_x the transverse wave number. Using well-known expressions for the reflection coefficient (RC) $R(\omega, k_x)$ (2a) and transmission coefficient (TC) $T(\omega, k_x)$ (2b), we can find the dependence of the reflected $r(\tau, x)$ and transmitted $t(\tau, x)$ wave packets, respectively. For example, for the reflected wave packet, we have:

$$r(\tau, x) = \frac{1}{4\pi^2} \int_{-\infty}^{\infty} \int_{-\infty}^{\infty} R(\omega, k_x) F(\omega, k_x) \exp(i\omega\tau - ik_x x) d\omega dk_x$$

Phase $\varphi(\omega, k_x) = \arg(R(\omega, k_x))$ can be represented as a series in powers $(\omega - \omega_0)$ and $(k_x - k_{x0})$ [9, 17]:

$$\begin{aligned} \varphi(\omega, k_x) = & \varphi(\omega_0, k_{x0}) + (\omega - \omega_0) \left(\frac{\partial \varphi(\omega, k_x)}{\partial \omega} \right)_{\substack{\omega=\omega_0 \\ k_x=k_{x0}}} \\ & + (k_x - k_{x0}) \left(\frac{\partial \varphi(\omega, k_x)}{\partial k_x} \right)_{\substack{\omega=\omega_0 \\ k_x=k_{x0}}} + \dots \end{aligned} \quad (3)$$

If the spectrum of the wave packet is concentrated near the center frequency ω_0 and wave number k_{x0} , then it can be considered a

quasimonochromatic highly directed group of waves. By limiting in (3) with the zero and first order terms and considering that at the spectrum width the reflection coefficient absolute value changes but little, $|R(\omega, k_x)| \approx \text{const}$, the packet group delay (GD) can be determined as the frequency derivative of the reflection (transmission) coefficient phase as in [9, 17]:

$$\Delta\tau_g(\omega_0, k_x) = - \left(\frac{\partial\varphi(\omega, k_x)}{\partial\omega} \right)_{\omega=\omega_0}. \quad (4)$$

The wave packet group shift (GS) is similarly introduced, provided that the wave packet is paraxial and highly directional one [12]:

$$\Delta x_g(\omega, k_{x0}) = \left(\frac{\partial\varphi(\omega, k_x)}{\partial k_x} \right)_{k_x=k_{x0}}. \quad (5)$$

For overcoming the discontinuity of a formally determined phase, the reflected packet group delay time (4) and group shift (5) are convenient to calculate through derivatives of the real and imaginary parts of the reflection coefficient, viz.

$$\Delta\tau_g(\omega_0, k_x) = \left(|R(\omega, k_x)|^{-2} \left[\text{Im}(R(\omega, k_x)) \frac{\partial}{\partial\omega} \text{Re}(R(\omega, k_x)) - \text{Re}(R(\omega, k_x)) \frac{\partial}{\partial\omega} \text{Im}(R(\omega, k_x)) \right] \right)_{\omega=\omega_0}$$

Similarly, according to (5), GS of the wave packet can be written as:

$$\Delta x_g(\omega, k_{x0}) = \left(|R(\omega, k_x)|^{-2} \left[-\text{Im}(R(\omega, k_x)) \frac{\partial}{\partial k_x} \text{Re}(R(\omega, k_x)) + \text{Re}(R(\omega, k_x)) \frac{\partial}{\partial k_x} \text{Im}(R(\omega, k_x)) \right] \right)_{k_x=k_{x0}}$$

Group shift and group delay are differential estimates, which determine the maximum shift and packet delay through the known reflection characteristics of the structure.

It will be observed that formulas Equations (4) and (5) characterize the packet delay time and shift only in the case when the displacements of all parts of the packet are equal, i.e., the packet propagates as a whole. Otherwise, the next term in expansion (3) which describes the group delay and group shift dispersion cannot be neglected. Generalizing, we may say that the account for the n terms of expansion (3) is sufficient to fulfill the condition $\varphi_\omega^{(n)}(\omega_0, k_{x0})/\varphi_\omega^{(n-1)}(\omega_0, k_{x0}) \ll T$ and $\varphi_{k_x}^{(n)}(\omega_0, k_{x0})/\varphi_{k_x}^{(n-1)}(\omega_0, k_{x0}) \ll L$, where T is the incident packet duration, L is the extent of the packet [17].

2.3. Integral Parameters of Wave Packet

For the wave packets distortion and fuzziness, we may introduce the delay time for each part of the packets: maximum, front, tail, etc. Let us consider the packets energy center mass delay (CMD) and center mass shift (CMS). The packet delay (or energy center delay) CMD and packet shift (or energy center shift) CMS can be calculated as the first order ordinary initial mathematical moment [9]:

$$\Delta x'_e = \int_{-\infty}^{+\infty} \int_{-\infty}^{+\infty} x S(\tau, x) dx d\tau, \tag{6}$$

$$S(\tau, x) = |s(\tau, x)|^2 / \int_{-\infty}^{+\infty} \int_{-\infty}^{+\infty} |s(\tau, x)|^2 dx d\tau$$

where $s(\tau, x)$ is the envelope surface of the packet under consideration. The quantity $\Delta x'_e$ determines the Goos-Hänchen shift, and for highly directional wave packets it coincides with differential estimate Δx_g given by (5). Similarly to CMD, the wave packet CMS we introduce in the following form:

$$\Delta \tau'_e = \int_{-\infty}^{+\infty} \int_{-\infty}^{+\infty} \tau S(\tau, x) dx d\tau \tag{7}$$

In the general case, the time delay $\Delta \tau'_e$ in Equation (7) and shift $\Delta x'_e$ in Equation (6) do not characterize the energy transport velocity and they are a sort of effective estimate of a packet delay and shift. Only in the case when the linear approximation holds and the wave packet form is unchanged, the time $\Delta \tau'_e$ and $\Delta \tau_g$, and also shift $\Delta x'_e$ and Δx_g values coincide and correspond to the energy transport velocity.

Let the packet duration σ'^2_τ and extent σ'^2_x be introduced as the second order central moment to quantitatively estimate the width of reflected and transmitted packet:

$$\sigma'^2_\tau = \int_{-\infty}^{+\infty} \int_{-\infty}^{+\infty} (\tau - \Delta \tau_e)^2 S(\tau, x) dx d\tau$$

$$\sigma'^2_x = \int_{-\infty}^{+\infty} \int_{-\infty}^{+\infty} (x - \Delta x_e)^2 S(\tau, x) dx d\tau \tag{8}$$

The shift and delay of the reflected and transmitted wave packets will be considered with respect to the corresponding parameters of the incident packet:

$$\Delta x_e = (\Delta x'_e - \Delta x_{init}) / \lambda_0, \quad \Delta \tau_e = (\Delta \tau'_e - \Delta \tau_{init}) f_0, \quad (9)$$

where Δx_{init} and $\Delta \tau_{init}$ are the delay and shift of initial packet. Instead of packet width (8) we considered wave packet widening (duration or extent with respect to the incident packet):

$$\sigma = \sigma' / \sigma_{init} - 1, \quad (10)$$

where σ' is the width of reflected (transmitted) packet and σ_{init} the width of initial packet. Thus, positive value of σ corresponds packet widening, but negative value of σ corresponds packet narrowing. It is clear that the method of determining the parameters of the wave packet shape distortion with the different order mathematical moments is meaningful only for the case when the corresponding integrals Equations (6)–(8) converge. For the wave packets limited in time domain and space, this condition is fulfilled by itself.

3. THE REFLECTION OF THE WAVE PACKETS FROM ASYMMETRIC BRAGG RESONATORS

A Fabry-Perot interferometer is typically made of a transparent plate with two reflecting surfaces, or two plane parallel highly reflecting mirrors. We can introduce Bragg resonators as Fabry-Perot interferometers with Bragg mirrors; however the thickness of the resonant transparent layer is equal to the half of Bragg wavelength. If Bragg mirrors have the same number of layers, one has a symmetric Bragg resonator. In opposite case the resonator is asymmetric one. For numeric simulation the structure with $M = 25$ layers was chosen, permittivity of layers was $\varepsilon_{2n-1} = 2$ and $\varepsilon_{2n} = 1$, respectively, and permeability was $\mu_{2n-1} = 1$, $\mu_{2n} = 1$, electrical thickness of layers was $h_n \sqrt{\varepsilon_n} = \lambda_0 / 4$. Let us consider the transformation of wave packet shape at oblique incidence for asymmetric Bragg resonators (Figure 1) than layer with resonance thickness has asymmetric location and its number was 15 (Figure 1(b)) or 11 (Figure 1(c)). For comparison structures of incident packet (Figure 1(a)) and one reflected from symmetric resonator (Figure 1(d)) are also presented.

The incident wave packet with π -cosinusoidal envelope is given by the following expression (Figure 1(a)):

$$f(\tau, x) = (\Phi(\tau + a) - \Phi(\tau - a)) (\Phi(x + b) - \Phi(x - b)) \cos(\pi\tau/2a) \cos(\pi x/2b) \sin(\omega\tau - k_x x),$$

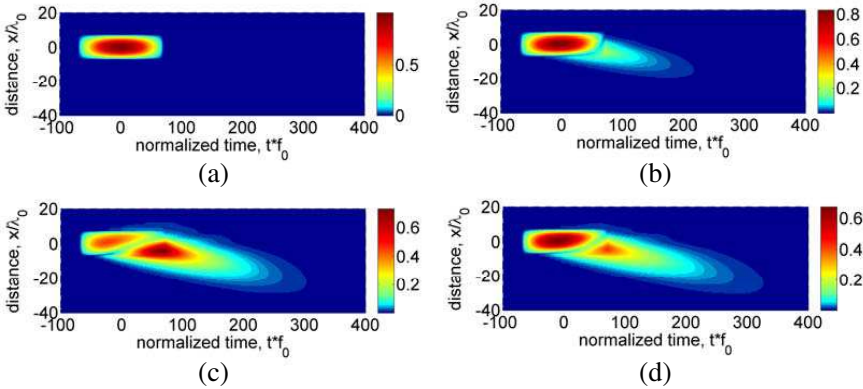


Figure 1. The reflection of the wave packet from Bragg resonators: (a) is the envelope of incident wave packet; (b) is the wave packet envelope reflected by an asymmetric Bragg resonator with far location of the resonance layer; (c) is the wave packet envelope reflected by an asymmetric Bragg resonator with near location of the resonance layer; (d) is the wave packet envelope reflected by symmetric Bragg resonator.

where Φ is the Heaviside step-function, a the absolute packet duration, and b the absolute extent of the wave packet.

In the case of reflection from the Bragg resonator, the wave packet is formed by two partial packets. One of them is reflected from the front face of the resonator but another is reflected from the back mirror formed by the back reflector. These partial packets are in antiphase due to satisfaction of the Bragg resonance conditions $h_m \sqrt{\varepsilon_m - \sin^2 \theta} = \lambda_0/2$, where m is the number of resonance layer. Calculations are based on the standard algorithm for the discrete Fourier transform [18]. Discretization parameters of wave packet had following values: $N_\tau = 2000$ is the number of samples in the time-domain, $N_x = 500$ is the number of samples in the space, $d\tau f_0 = 0.17$ is the sampling step in the time-domain, and $dx/\lambda_0 = 0.5$ is the sampling step in the space. The initial incident wave packet with TE polarization (Figure 1(a)) had length of $b = 7$, duration of $a = 70$, incident angle was determined by $k_x/k_0 = 0.1$ ($\theta \approx 5.7$ degrees) and the carrier frequency was $f/f_0 = 1.005$. If the resonator is symmetric, the delay and the shift of the reflected wave packet are always positive, and in the case of $m = 13$, the parameters have got the values: delay $\Delta\tau_e = 20.03$, shift $\Delta x_e = 1.46$, time widening $\sigma_\tau = 1.13$, space widening $\sigma_x = 0.79$. Moreover, as can be seen from

Figure 1(d) the wave packet has been split and has two parts localized as in time domain so in space one. The first local part has the largest amplitude and has greater part of energy. For asymmetric resonator with $m = 11$ (Figure 1(c)) the value of CMD has been $\Delta\tau_e = 52.24$ and CMS has been $\Delta x_e = 4.25$. They have been greater than ones in the case of the symmetric resonator. The splitting of the wave packet also appears upon reflection of asymmetric Bragg resonator. For asymmetric resonator with far location of the resonance layer with $m = 15$ (Figure 1(b)) the CMD value for reflected packet has become negative $\Delta\tau_e = -0.24$, the CMS has been $\Delta x_e = 0.03$, estimates of widening have been $\sigma_\tau = 0.17$, $\sigma_x = 0.11$.

The symmetric Bragg resonators, even with small number of layers, have high Q -factor (it has been defined as $Q = f'/2f''$ where f' is the real part of resonance frequency and f'' is the imaginary one), thus GD and GS of reflected packet become large for them (Figures 2(a)–(b), line 1) if the condition of proximity of the carrier frequency and the incidence angle to value of Bragg resonance is fulfilled. The Q -factor of the asymmetric resonator is always lower than corresponding one for the symmetric resonator but GD and GS is being as smaller so larger in comparison with ones for the symmetric resonator. In the vicinity of Bragg resonance angle or (and) frequency, GD and GS of reflected packet take either large positive (Figures 2(a)–(b), line 2) or large negative (Figures 2(a)–(b), line 3) values. The frequency intervals with negative value of GD and GS are observed only for asymmetric resonators and always located near the resonance frequency or angle of incidence (Figures 2(a)–(b), line 3).

Let us consider the variation of CMD and CMS (or Goos-Hänchen shift), and widening of the wave packet with π -cosinusoidal envelop

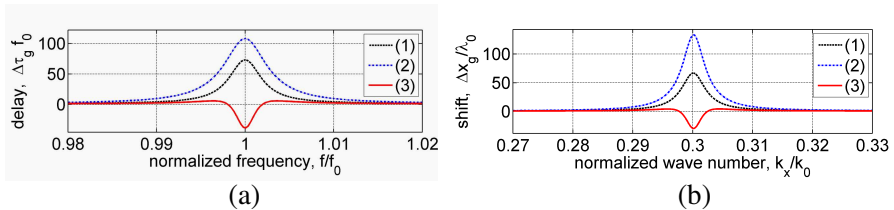


Figure 2. Group delay (GD) and group shift (GS) of reflected wave packet: (a) GD and (b) GS in cases of symmetric Bragg resonator with $m = 13$ (line 1), asymmetric Bragg resonator with near location of resonance layer with $m = 11$ (line 2), and asymmetric Bragg resonator with far location of resonance layer when $m = 15$ (line 3); total number of layers of the Bragg resonator is $M = 25$.

versus the carrier frequency and angle of the incidence under reflection from asymmetric Bragg resonator with far resonance layer location. And also we will compare differential and integral parameters of delay and shift for wave packets with different duration and extent. The resonator parameters are the same as for case presented in Figure 1. At the first let us analyze the delay of the wave packet at normal incidence $k_x/k_0 = 0$ ($\theta = 0$ degrees) (Figure 3(a), lines 1–3). When the duration of the packet has been $a = 75$ (Figure 3(a), line 1), in the vicinity of the Bragg resonance CMD has take small negative values and this packet simultaneously has become wider along the time axis (Figure 3(b), line 1). With increasing packet duration up to $a = 150$ (Figure 3(a), line 2), at the Bragg resonance frequency CMD has been approaching to the group delay $(\Delta\tau_g - \Delta\tau_e)/\sigma_{init} \approx 0.406$ (Figure 2(a), line 3), and the widening σ_τ has had non-monotonic frequency dependence near the Bragg resonance. For packet duration $a = 300$ in the Bragg reflection band CMD and GD response coincide with greater accuracy (on the Bragg frequency $(\Delta\tau_g - \Delta\tau_e)/\sigma_{init} \approx 0.074$), and besides reflected packet has had shorter duration (Figure 3(b), line 3).

And now let us proceed to the analysis of shift of the wave packet with duration $a = 100$ versus angle of incidence for variation of packet

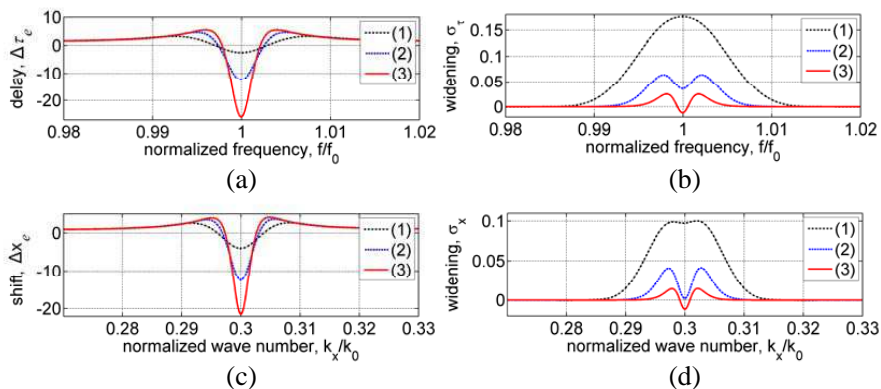


Figure 3. Parameters of delay, shift and widening of reflected wave packets: (a) CMD and (b) widening of reflected wave packet with extent $b = 15$ at normal incidence for the Bragg resonator with the far location of the resonance layer, line 1 for duration $a = 75$, line 2 for $a = 150$, line 3 for $a = 300$; (c) CMS and (d) space widening of reflected wave packet with duration $a = 100$ for the Bragg resonator with the far resonance layer location, line 1 for extent $b = 75$, line 2 for $b = 150$, line 3 for $b = 300$.

extent and compare these values with the values of group shift. Carrier frequency of the packet was $f/f_0 = 3.1$, as in the previous case, the structure was asymmetric Bragg resonator with far location of resonance layer. Negative (anomalous) shift values have been observed at the angles of incidence in the vicinity of $k_x/k_0 \approx 0.3$ ($\theta \approx 17.5$ degrees) (Figure 3(c)). When the spatial extent of the incident packet was $b = 75$, reflected packet became broader (Figure 3(d), line 1) and had a small negative shift (Figure 3(c), line 1). This value of the mass center shift corresponds to anomalous Goos-Hänchen effect. Further with increasing the extent of packet to $b = 150$, the negative shift increases (Figure 3(c), line 2), and the widening near the angle of Bragg resonance became a sharply nonmonotonic behavior (Figure 3(d), line 2). If the width of packet increased to the value of $b = 300$, the reflected packet became narrower (Figure 3(d), line 3), and the integral (CMS) and differential (GS) estimates have close values $(\Delta x_g - \Delta x_e)/\sigma_{init} \approx 0.079$ (Figure 3(c), line 3).

For single incident wave packet the reflected wave packet is formed by two antiphase wave packets corresponding to reflections from the front and back mirrors. Even if the reflected wave packet consists of two parts, under condition of a rather narrow spectrum of the initial packet and corresponding essential overlapping of reflected packets they form integral whole packet. Under the last condition, CMD and CMS can take negative values if the reflection from the front mirror is dominant in comparison with the reflection from the back mirror. If the reflectivity of the back mirror reduces because of decreasing the number of layers in it, the center of mass of the reflected package is moving ahead of the position of the center of mass for the initial resonator. The similar effect can be observed under increasing the reflectivity of the front mirror. This phenomenon occurs in a number of numerical simulations with various numbers of layers in mirrors.

Summarizing, we can say that when the layer with resonance thickness has asymmetric location with respect to the edges of the structure and it is closer to the front $m < (M + 1)/2$ (near location of resonance layer), CMD and CMS are always positive, otherwise, when the layer of resonance thickness is closer to the end of the structure and $m > (M + 1)/2$ (far location of resonance layer) CMD and CMS can take negative values if the frequency and angle of incidence are in vicinity of Bragg resonance for the packets with the duration and extent which provide a rather narrow spectrum. This effect occurs if reflections from the front and back mirrors can not be observed separately.

According to the packet's GD and CMD, GS and CMS definitions, it is clear that they can take any value: either positive or negative,

that gives the value of speed larger or smaller than the speed of light in vacuum. The negative GD and GS values do not in any way conflict with the special relative theory and do not violate the causality principle, as in the general case, they do not correspond either to the energy transmission, or to the signal propagation. For carrier frequency and angle of incidence belonging to the frequency and angle intervals where GD and GS possess either negative values or values corresponding to the superluminal propagation, the form of informative packets (signals) is strongly distorted. Thus, application of GD and GS, which have been defined for the condition of packet shape constancy, as an estimate of signal propagation parameters is incorrect in the vicinity of such values of frequency or angle of incidence.

Analytical closed form for widening response can be computed only for simple cases of reflectors (with simple dispersion) and trivial wave packet envelope. For Bragg reflectors and casual (space-time limited) wave packets with smooth envelope we have to use the numerical calculation for obtaining of widening estimates.

The packet CMD and CMS can also take on anomalous values if losses or amplification are present. In this case, along with the incident packet center of mass it is convenient to consider the center of losses (or center of amplification). Following to [9], let the center of losses be considered as a loss-power packet energy center. The center of amplification is introduced similarly. Then, in dependence on the relationship between positions of the packet center of mass and the center of losses in the time-space plane, the reflected (transmitted) packet CMD and/or CMS will possess either positive or negative values. For example, the CMD is negative in case, when in the time domain the center of losses follows the center of mass of a packet propagating in vacuum. In case of amplification, the CMD takes negative value, when the center of amplification advances the packet center of mass [9, 10].

4. TRANSMISSION OF WAVE PACKETS THROUGH THE QUASIPERIODIC APODIZED BRAGG STRUCTURE

In this section, we consider the quasiperiodic apodized Bragg structure, which is a structure with a smooth perturbation permittivity of one of the two layers that form the period. If the contrast of permittivity increases smoothly from the edges to the center of the structure in accordance with law $\varepsilon(n)$, then this type of perturbation of structure periodicity leads to the suppression of the side maxima (Figures 4(a)–(b), line 2 and line 3) in the frequency domain, as well as in the domain

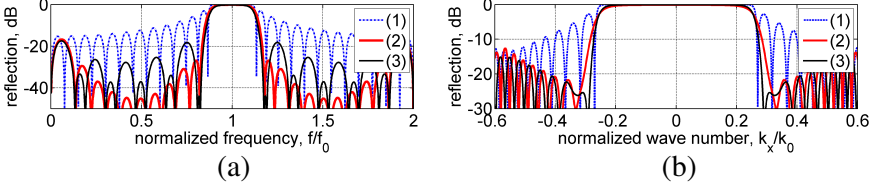


Figure 4. Reflection characteristics of apodized Bragg structure: (a) frequency response and (b) angle response of periodic reflector (line 1), quasiperiodic reflector with apodization law $\varepsilon(n) \sim \sin^2(n)$ (line 2), and quasiperiodic reflector with $\varepsilon(n) \sim \sin(n)$ (line 3).

of incidence angle [2, 6, 19].

Choice of an apodization function form is most often determined by specific tasks of application, such as the achievement of the lowest level of the first side lobe of reflection (transmission) band (Figure 4(a), line 3), or the maximum suppression of peaks in the interval between adjacent Bragg reflection bands (Figure 4(a), line 2). We have investigated apodized structure with total number of layers $M = 25$, permittivity of the even layers $\varepsilon_{2n} = 1$ geometrical thickness $h_{2n} = 0.25\lambda_0$, and the parameters of the odd layers for line 3 in Figure 4(a), and Figure 4(b) are $\varepsilon_{2n-1} = 1 + \sin(\pi(2n-1)/(M+1))$, $h_{2n-1} = 0.25\lambda_0/\sqrt{\varepsilon_{2n-1}}$, for line 2 in Figure 4(a), and Figure 4(b) are $\varepsilon_{2n-1} = 1 + \sin^2(\pi(2n-1)/(M+1))$, $h_{2n-1} = 0.25\lambda_0/\sqrt{\varepsilon_{2n-1}}$. Apodization introduction leads to eigenoscillations quality factor decreasing, and the influence of apodization is stronger if the frequency closer to the center of the interval between adjacent Bragg reflection bands.

Further let examine transmitted packets of different duration and extent for periodic and quasiperiodic Bragg reflectors at normal incidence with the center frequency of a spectrum near the edge of the Bragg reflection band with value of $f/f_0 = 1.134$. For transmission through strictly periodic Bragg reflector ($M = 25$, $\varepsilon_{2n-1} = 2$, $\varepsilon_{2n} = 1$, $\mu_{2n-1} = 1$, $\mu_{2n} = 1$) relatively wide packet with $b = 15$ and with short duration of $a = 5$ has been split and has had two localized maximum, in addition, the packet has become broader with $\sigma_x = 0.0008$, delay of $\Delta\tau_e = 10.2075$, and its duration has become larger $\sigma_\tau = 2.5562$ (Figure 5(a)). The wave packet transmitted in case of quasiperiodic apodized reflector has had larger amplitude and less spreads $\sigma_x = 0.0003$, $\sigma_\tau = 0.3038$, and moreover, the delay has been much smaller $\Delta\tau_e = 7.1605$ (Figure 5(b)).

Further, let us consider the CMD and CMS, and also let us analyze deformation versus carrier frequency and angle of incidence for the

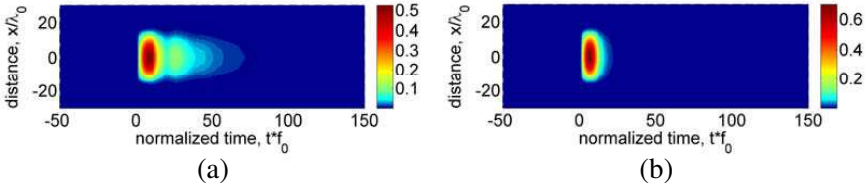


Figure 5. Transmission of wave packets through quasiperiodic apodized Bragg reflector: the wave packet ($a = 5$; $b = 15$) with the carrier frequency near the edge of the Bragg reflection band (a) for strictly periodic reflector, and (b) for quasiperiodic apodized reflector.

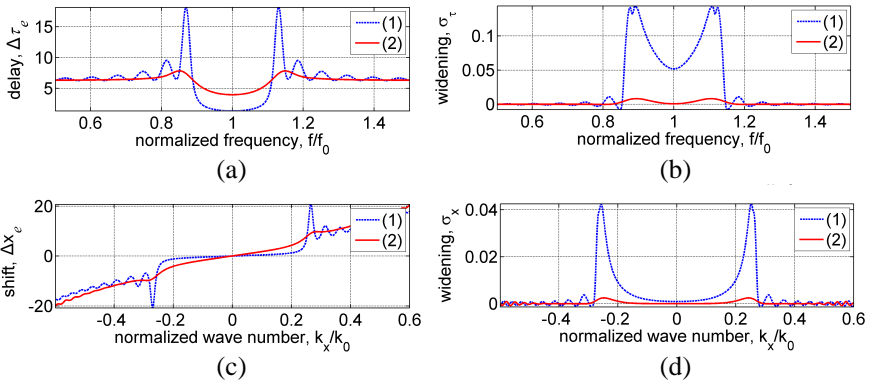


Figure 6. Parameters of delay, shift and widening of transmitted wave packets: (a) CMD and (b) widening of transmitted wave packet, $a = 30$ is the duration, $b = 15$ is the extent for normal incidence on a periodic Bragg reflector; (c) CMS and (d) space widening of transmitted wave packet with a carrier frequency $f/f_0 = 5$, $a = 30$ is the duration, $b = 15$ is the extent. (Line 1 for strictly periodic Bragg reflector and line 2 for quasiperiodic apodized Bragg reflector $\varepsilon_{2n-1} = 1 + \sin^2(\pi(2n - 1)/(M + 1))$.)

transmitted wave packets with initial duration of $a = 30$ and extent of $b = 15$ for quasiperiodic apodized Bragg reflector. In the Bragg reflection band for periodic Bragg reflector at the normal incidence transmitted wave packet has the value of CMD that corresponds exceeding the speed of light velocity propagation.

At the edges of the reflection frequency band, the center mass delay gains large value, much greater than the propagation time of packet for the free-space distance which is equal to the electrical

thickness of the structure (Figure 6(a), line 1). In the Bragg transmission frequency band the CMD slightly oscillates near the level which is determined by the propagation time of packet for the free-space distance which is equal to the electrical thickness of the structure (Figure 6(a), line 1). The wave packet widening takes maximum value at the edges of the Bragg reflection frequency band (Figure 6(b), line 1). Bragg structure apodization leads to more uniformly CMD frequency characteristic in the Bragg transmission band (Figure 6(a), line 2), and transmitted wave packet is much less distorted (Figure 6(b), line 2).

Similarly with the center mass delay, the center mass shift (Goos-Hänchen shift) of the wave packet transmitted through apodized Bragg reflector increases more smoothly (Figure 6(c), line 2), and the widening is much smaller (Figure 6(d), line 2) in comparison with the CMS and widening of wave packet transmitted through periodic Bragg reflector (Figure 6(d), line 1). Thus, the apodization implementation leads to reducing the space-time distortion of wave packets.

5. THE PULSES REFLECTION FROM QUASIPERIODIC CHIRP-APODIZED STRUCTURES

Let us consider the example of a specific structure with chirp variation of thickness of the “period” having characteristic properties of GD nonuniformity within a reflection band. We use quotation marks for the term period, because in opposite to the strictly periodic and quasiperiodic Bragg structures (Sections 3 and 4) the electric thickness of double-layer unit cell, forming a chirp structure is changed. In view of complexity which may arise in measurements, the number of structure layers is taken small namely $M = 13$, however it is sufficient that the expected phase behavior effects could be detected. The structure “period” consists of the polystyrene layer ($\varepsilon_{2n-1} = 2.2$, $\mu_{2n-1} = 1$) with the constant geometric thickness $h_{2n-1} = 0.8$ (mm) and the air layer ($\varepsilon_{2n} = 1$, $\mu_{2n} = 1$) with a chirp varying thickness $h_{2n} = 8 + 0.2(n - 1)$ and $h_{2n} = 9 - 0.2(n - 1)$ (in millimeters), where n is number of current “period”. Additionally, we introduce the deformation parameters such as pulse envelope skewness η and the coefficient of kurtosis ξ :

$$\eta_\tau = \int_{-\infty}^{+\infty} (\tau - \Delta\tau_e)^3 S(\tau) d\tau / \sigma_\tau^3, \quad (11)$$

$$\xi_\tau = \xi_{init} - \int_{-\infty}^{+\infty} (\tau - \Delta\tau_e)^4 S(\tau) d\tau / \sigma_\tau^4,$$

where ξ_{init} is the kurtosis coefficient of initial pulse.

Properly speaking, the linear variation of Bragg structure leads to destroying of Bragg reflection. But for weak disturbance of layer thickness and small total number of layers the reflection is strongly similar to Bragg one. This type of variation is also called chirp-podization. Now let us consider the pulse distortion with the π -cosinusoidal envelope and absolute duration $a = 10$ (ns) for the reflection from the given structure with chirp variation of thickness of the “period” in the directions toward the increase (Figures 7(a)–(d), line 1) and decrease (Figures 7(a)–(d), line 2) of the electrical thickness of the “period”.

In the Bragg reflection band, the CMD has monotonically decreased in the case of a linear increase of the “period” (Figure 7(a), line 1) and monotonically increased otherwise (Figure 7(a), line 2). Pulse widening and coefficient of kurtosis have been varying but just slightly within the Bragg reflection band and shown similar behavior either for the direct or inverse directions of variation of the “period” at the Bragg reflection band edges. However, at frequencies close to Bragg reflection band edges, the skewness has changed its sign remaining close to zero within the band if the direction of “period” growth has been changed (Figure 7(c), lines 1 and 2).

The structure with chirp variation of thickness of the “period”

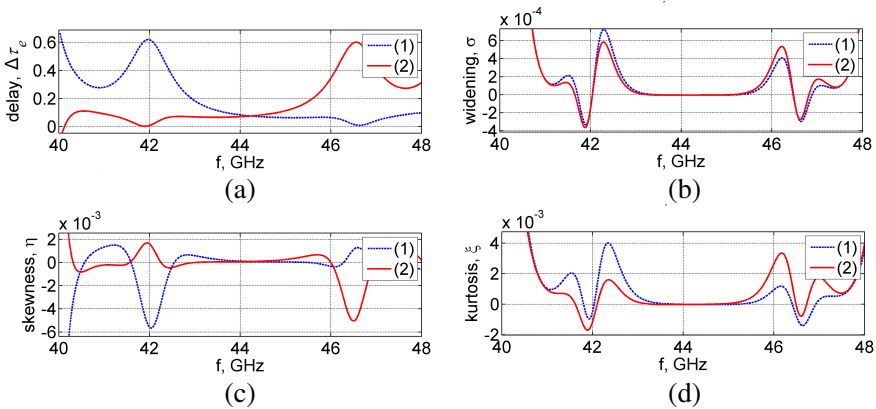


Figure 7. Reflected pulse distortion parameters: (a) time delay, (b) widening, the coefficients of (c) skewness and (d) kurtosis of a pulse with initially π -cosinusoidal envelope reflected from a layered structure of $M = 13$ layers with a linearly increasing (blue line 1) and decreasing (red line 2) thickness of the “period”.

described in the above mentioned example of investigation of CMD and pulse distortion with the π -cosinusoidal envelope in the case of reflection from a structure with chirp variation of thickness of the “period” was experimentally investigated. The pulse GD for reflection from the Bragg structure with small chirp variation of an electrical thickness of the “period” either monotonically increases or monotonically decreases (in the center of Bragg reflection band), similar to the CMD for such a structure. Then, if $-d\varphi_{dir}/d\omega$ was GD (measured in ns) for the reflection from a structure with increasing “period” (forward direction), and $-d\varphi_{inv}/d\omega$ was GD for the reflection from the structure with linearly decreasing “period” (inverse direction), the difference $d\varphi_{dir}/d\omega - d\varphi_{inv}/d\omega$ monotonically increases within the Bragg reflection band and passes through zero near the Bragg reflection frequency (Figure 8(a), line 2). The composition of the difference $d\varphi_{dir}/d\omega - d\varphi_{inv}/d\omega$ allowed us to obtain greater accuracy in detection of GD asymmetric behavior within the Bragg reflection band in measurements (Figure 8(a), line 1). Figure 8(b) shows the simulated (line 2) and measured (line 1) dependences of the squared absolute value of reflection coefficient for such a structure.

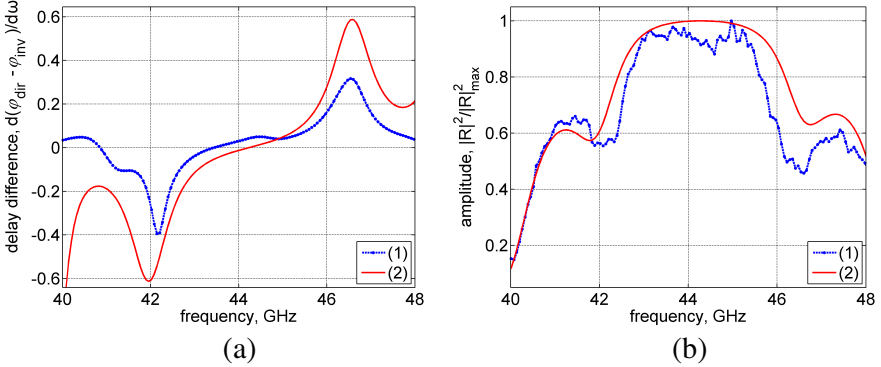


Figure 8. Frequency-response characteristics of pulse reflection from the structure with chirp variation of thickness of the “period”: (a) is the GD difference for the decrease and increase directions of the “period” $d(\varphi_{dir} - \varphi_{inv})/d\omega$, (b) is the squared absolute value of reflection coefficient. (Blue line 1 is the measured, while red line 2 the simulated data.)

The reflection coefficient phase-response characteristics were measured with the measuring-computer system [20] which employs the Fourier-holography principle within the frequency band 40–48 GHz. In making measurements, a pyramidal horn with the gain factor of

$G = 25$ dB was used that allowed us to carry out measurements at greater distance in the comparison with the case of open-ended waveguide radiator. Hence, investigation of structures with greater electrical thickness became possible [21]. The reference signal was the reflection from the horn throat. The distance from the horn throat to the front edge of investigated structure was 420 mm. According to [21], in the time signal synthesized by inverse Fourier-transform of the data measured in frequency domain there are the autocorrelation function (ACF) of time dependence of reflection from investigated structure and the cross-correlation function (CCF) of this reflection and the reference signal. The CCF keeps the information about the structure phase characteristics, but because of essential reference signal dependence on frequency the determination of frequency dependence of the squared absolute value of reflection coefficient is accompanied by significant distortions, while the ACF allows us to determine it with sufficient precision. The useful signal can be separated in the time domain by a window under condition that the corresponding CCF and ACF belong to different time intervals and are not overlapping each with other [21]. In Figure 8(a) the experimentally obtained phase against frequency is presented by line 1. This phase has been calculated by discrete Fourier-transform of the part of time-domain synthesized signal under preceding extraction of CCF by windowing. One can observe the analogous behavior of calculated (line 2) and experimentally obtained data.

Different from [21], the squared absolute value of the reflection coefficient (Figure 8(b), line 1) was calculated with Prony's method [22]. This method is a numerical algorithm of the determination of the complex-valued factors of exponents and the corresponding magnitude factors for data given in equidistant points if the data can be represented as a sum of exponential components. The frequency dependence of the reflection coefficient of the layered structure satisfies the mentioned requirements [12, 23]. Prony's algorithm was performed with the use of the moving rectangular window with size of $w = 13$ samples and for order of model of $q = 3$. Squared absolute value of the reflection coefficient was estimated as modulus of magnitude factors of exponential component with zero-valued exponent. This set of exponents can be considered as function of frequency due to implementation of moving window in frequency domain. This approach has an advantage over the method of ACF extraction by time-domain windowing and successive Fourier transform for obtaining reflection coefficient dependence versus frequency. This effect is determined by elimination of influence of the window edges as in frequency domain so in time one (so-called the Gibbs phenomenon).

6. CONCLUSION

GD and GS packet negative values are inherent to asymmetric Bragg resonators and observed under the condition that a resonance thickness layer is located closer to the end of a structure, $m > (M + 1)/2$. For case of large wave packet durations and extent, integral and differential packet estimates take approximately equal values. CMD and CMS have anomalous values via packet distortions: widening, variation of asymmetry, coefficient of kurtosis.

Significant relative reduction of the side maximum level can be achieved by spatial permittivity contrast apodization of multilayer structures. It provides a much smaller distortion of the reflected or transmitted wave packet with the angle of incidence and carrier frequency near the edge of the Bragg band reflection in comparison with similar periodic structures.

Experimentally obtained phase-response and amplitude-frequency response characteristics of layered structures with a chirp varying thickness of the “period” have confirmed GD and CMD behavior that has been obtained by calculation with the harmonic wave expansion and transmission matrix methods. GD and CMD determination permits to obtain negative values and those corresponding to propagation velocities exceeding the speed of light. For the pulses with insufficient frequency localization, neither GD nor CMD can be used as a unique estimate of delay time of the transmitted and reflected pulses under Bragg structures irradiation.

REFERENCES

1. Elachi, C., “Waves in active and passive periodic structures: A review,” *Proceedings of the IEEE*, Vol. 64, No. 12, 1666–1698, 1976.
2. Yariv, A. and P. Yeh, *Optical Waves in Crystals: Propagation and Control of Laser Radiation*, Wiley, New York, 2002.
3. Kusiek, A., R. Lech, and J. Mazur, “Hybrid technique for the analysis of scattering from periodic structures composed of irregular objects,” *Progress In Electromagnetics Research*, Vol. 135, 657–675, 2013.
4. Wu, J.-J., D. Chen, K.-L. Liao, T.-J. Yang, and W.-L. Ouyang, “The optical properties of Bragg fiber with a fiber core of 2-dimension elliptical-hole photonic crystal structure,” *Progress In Electromagnetics Research Letters*, Vol. 10, 87–95, 2009.
5. Tuz, V. R., S. L. Prosvirnin, and V. B. Kazanskiy, “Mutual conversion of TM_{mn} and TE_{mn} waves by periodic and aperiodic

- waveguide filters composed of dense metal-strip gratings,” *Progress In Electromagnetics Research B*, Vol. 30, 313–335, 2011.
6. Borulko, V., O. Drobakhin, and D. Sidorov, “Eigenfrequencies of periodic and quasiperiodic apodized Bragg structures,” *Telecommunications and Radio Engineering*, Vol. 71, No. 16, 1433–1445, 2012.
 7. Liu, Y. and Z. Lu, “Phase shift defect modes in one-dimensional asymmetrical photonic structures consisting of two rugate segments with different periodicities,” *Progress In Electromagnetics Research*, Vol. 112, 257–272, 2011.
 8. Matuschek, N., F. Kartner, and U. Keller, “Theory of double-chirped mirrors,” *IEEE Journal of Selected Topics in Quantum Electronics*, Vol. 4, No. 2, 198–208, 1998.
 9. Vainshtein, L. A., “Propagation of pulses,” *Sov. Phys. Usp.*, Vol. 19, 189–205, 1976.
 10. Kopfermann, H. and R. Ladenburg, “Untersuchungen über die anomale dispersion angeregter Gase V. Teil: Negative dispersion in angeregtem Neon,” *Zeitschrift für Physik A Hadrons and Nuclei*, Vol. 65, No. 3–4, 167–188, 1930.
 11. Bass, F. and L. Resnick, “Wave beam propagation in layered media,” *Progress In Electromagnetics Research*, Vol. 38, 111–123, 2002.
 12. Wait, J. R., *Electromagnetic Waves in Stratified Media*, Pergamon Press, Oxford, 1970.
 13. Born, M. and E. Wolf, *Principles of Optics*, Pergamon Press, Oxford, 1975.
 14. Tuz, V. R., “Three-dimensional Gaussian beam scattering from periodic sequence of bi-isotropic and material layer,” *Progress In Electromagnetics Research B*, Vol. 7, 53–73, 2008.
 15. Ivanov, O. V. and D. I. Sementsov, “Negative shift of light beam reflected from the interface between optically transparent and resonant media,” *Optics and Spectroscopy*, Vol. 89, No. 5, 737–741, 2000.
 16. Kandic, M. and G. E. Bridges, “Limits of negative group delay phenomenon in linear causal media,” *Progress In Electromagnetics Research*, Vol. 134, 227–246, 2013.
 17. Ginzburg, V. L., *Propagation of Electromagnetic Waves in Plasma*, Pergamon Press, Oxford, 1970.
 18. Oppenheim, A. V. and R. W. Schaffer, *Discrete-time Signal Processing*, 619, Prentice-Hall, 1989.
 19. Sun, N.-H., J.-J. Liao, Y.-W. Kiang, S.-C. Lin, R.-Y. Ro, J.-

- S. Chiang, and H.-W. Chang, "Numerical analysis of apodized fiber Bragg gratings using coupled mode theory," *Progress In Electromagnetics Research*, Vol. 99, 289–306, 2009.
20. Alekseev, V., O. Drobakhin, Ye. Kondrat'yev, and D. Saltykov, "Microwave introscopy using multifrequency measurements and transversal scan," *IEEE Aerospace and Electronic Systems Magazine*, Vol. 21, No. 2, 24–26, 2006.
 21. Antropov, O. S., V. F. Borulko, O. O. Drobakhin, and S. M. Vovk, "Nonquadratic regularization procedure for multifrequency amplitude data extrapolation in microwave introscopy of dielectric structures Fourier-holography applications," *Telecommunications and Radio Engineering*, Vol. 68, 905–913, 2009.
 22. Hildebrand, F. B., *Introduction to Numerical Analysis*, McGraw-Hill, New York, 1956.
 23. Brekhovskikh, L. M., *Waves in Layered Media*, Academic Press, New York, 1960.